

Diffusion accelerates and enhances chirality selectionRyo Shibata, Yukio Saito,^{*} and Hiroyuki Hyuga[†]*Department of Physics, Keio University, Yokohama 223-8522, Japan*

(Received 15 March 2006; revised manuscript received 30 May 2006; published 23 August 2006)

The diffusion effect on chirality selection in a two-dimensional reaction-diffusion model is studied by Monte Carlo simulations. The model consists of achiral reactants A which turn into either of the chiral products R or S in a solvent of chemically inactive vacancies V . The reaction contains a nonlinear autocatalysis as well as a recycling process, and the chiral symmetry breaking is monitored by an enantiomeric excess (ee) ϕ . Without dilution a strong nonlinear autocatalysis ensures chiral symmetry breaking. By diluting a diffusionless system, the ee ϕ decreases and a racemic state is recovered below a critical concentration c_c . When the diffusion is allowed, the steady value of ϕ increases and c_c decreases. As for the relation between the ee ϕ and the concentration c , a formula interpolating between the diffusionless ($D=0$) and the homogeneous ($D=\infty$) limits is proposed by incorporating the diffusional enhancement of the concentrations of chiral species. Diffusion also accelerates the development of the chiral order, and the time required to establish the order in a system of a size L^2 is inversely proportional to the diffusion constant D as L^2/D .

DOI: [10.1103/PhysRevE.74.026117](https://doi.org/10.1103/PhysRevE.74.026117)

PACS number(s): 82.40.Ck, 05.90.+m, 05.50.+q

I. INTRODUCTION

It has long been known that natural biomolecules choose one type of an enantiomer among two possible stereostructures and the chiral symmetry is broken in life: Amino acids in proteins are all L-type, while sugars in nucleic acids are all D-type [1–3]. There are many studies of the origin of this homochirality, but the asymmetry caused by various proposed mechanisms turned out to be very minute [4–6]. Frank found more than 50 years ago that a linear autocatalysis accompanied by a mutual inhibition is necessary in an open system for the amplification of the enantiomeric excess (ee) of one type [7]. The model with enantiomeric cross inhibition is extended to polymerization models [8,9]. Experimental realization of the ee amplification is found recently in pyrimidyl alkanol [10] and explained by a nonlinear autocatalytic process in a closed system [11,12]. The addition of a recycling process to this nonlinear system is shown to realize an asymptotic selection of a unique chiral state [13]. So far, we know no chemical reaction system with a recycling process, but an open-flow system with catalytic chiral polymers is shown to be cast in a recycling model [14]. The importance of the recycling process is also shown in nonautocatalytic but a polymerization-epimerization model [15].

All the above arguments assume that the reaction takes place homogeneously. For spatially extended systems, however, the inhomogeneity affects the symmetry breaking in general. In condensed matter systems, for instance, elements are located densely in contact with each other and interactions propagate through neighboring elements so as to cause coherent phase transitions in a macroscopic system [16]. In contrast to equilibrium symmetry breaking in condensed matter, organic molecules in the primordial era might have been distributed dilutely in a solution. If this were the case, molecular transport is necessary in order to bring molecules

into contact to activate autocatalysis. In a previous paper [17] we briefly reported the diffusion effect on the chiral symmetry breaking by means of Monte Carlo simulations. Later the effect is studied for a slightly different chemical reaction model by numerically solving partial differential equations [18].

Here we give a detailed Monte Carlo simulation study of the diffusion effect on the chirality proliferation in an extended system. After introducing the model and Monte Carlo simulation algorithm in Sec. II, we consider first the chirality selection in a diffusionless system and point out some similarity of the present chemical reaction system to the Ising ferromagnet in Sec. III [16,19–21]. There, the effect of site dilution is also discussed. In Sec. IV, the diffusion effect is studied systematically and the chiral symmetry breaking is found to be enhanced by the diffusion. With a larger diffusion constant, the chiral order develops faster and the enantiomeric excess ϕ reaches to a higher magnitude. The value of the critical concentration where the chiral order completely disappears decreases as well. The speeding up of the chiral order proliferation is in accordance with the previous study of the partial differential equations [18]. The enhancement in the saturation value of the chirality as well as the shrinkage of the racemic region is qualitatively interpreted in such a way that the diffusion effectively increases the concentrations of chemically active molecules and consequently promotes autocatalysis. The idea is summarized in a simple interpolation formula as for the diffusion coefficient dependence of the order parameter and the concentration relation. The study is summarized in Sec. V.

II. MODEL AND SIMULATION ALGORITHMS

The model we study is essentially the same as the one proposed in the previous paper [17]. There are four types of molecules: an achiral reactant A , two types of product enantiomers R and S , and a solvent molecule in a diluted system, which we call a vacancy V . Molecules are treated as entities which occupy square lattice sites and can move randomly

^{*}Electronic address: yukio@rk.phys.keio.ac.jp[†]Electronic address: hyuga@rk.phys.keio.ac.jp

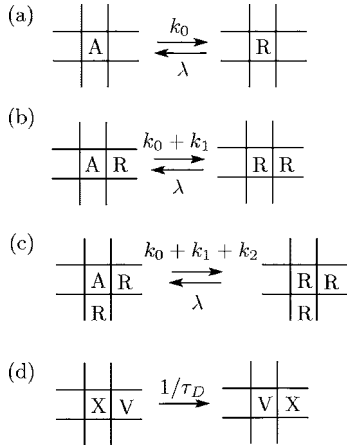


FIG. 1. Various processes with transition probabilities: (a) non-autocatalytic, (b) linearly autocatalytic, (c) nonlinearly autocatalytic reactions with recycling, and (d) a vacancy diffusion. X in the diffusion process (d) represents chemically active species A , R , or S .

thereon. Double occupancy of a lattice site is forbidden. On a square lattice of a size L^2 , periodic boundary conditions are imposed in both x and y directions.

Various processes in the system are summarized in Fig. 1. An isolated achiral reactant A turns into a chiral R or S molecule with a rate k_0 , as in Fig. 1(a). When there is one R (S) molecule in the nearest neighbor of a reactant A , the production rate of R (S) increases by an additional linear autocatalytic rate k_1 , as in Fig. 1(b). When there are two or more R 's (S 's) in the nearest neighborhood, the production rate of R (S) is further enhanced by an additional nonlinear autocatalytic rate k_2 , as in Fig. 1(c). The rate of back reaction, λ , is assumed constant, independent of the environment around chiral molecules R or S [Figs. 1(a)–1(c)]. By these chemical reaction processes, the number densities a , r , and s of active molecules A , R , and S vary, but the total number density of active molecules, $a+r+s=c$, is fixed constant, reflecting the assumption of a closed system corresponding to the Soai reaction [10]. The degree of chiral symmetry breaking is represented by the ee order parameter

$$\phi = \frac{r-s}{r+s}. \quad (1)$$

A vacancy V is inactive as for the chemical reaction, but plays a vital role in the diffusion process. When chemically active species A , R , and S are neighboring to V , they exchange their sites with V randomly with a lifetime τ_D , as in Fig. 1(d). The diffusion coefficient is then $D=a^2/(4\tau_D)$ with a being the lattice constant and set to be unity hereafter. Previously we simulated only the case with $D=1/4$, because the Metropolis algorithm was used in the Monte Carlo simulation [17]. In the present paper we want a systematic study of diffusion effect on the chirality selection, and therefore an arbitrary variation of the diffusion coefficient D is necessary. For that purpose, we adopt a waiting time algorithm for the Monte Carlo simulation.

The simulation runs as follows: All the positions which can undertake a process i are tabulated in a list; every site in

the list has the same transition probability P_i to perform the reaction or diffusion process i , shown in Fig. 1. Assume that there are n_i lattice sites in the corresponding list of the process i . Then, the total probability of events in a unit time is obtained as $P_{\text{tot}}=\sum_i P_i n_i$. In other words, in a time interval $dt=1/P_{\text{tot}}$, one of the process takes place on average. By generating a quasirandom number x which is uniformly distributed between 0 and P_{tot} , the process j which satisfies the condition

$$\sum_{i=1}^{j-1} P_i n_i \leq x < \sum_{i=1}^j P_i n_i \quad (2)$$

is to be performed. The lattice site which performs the process j is listed at the k th position in the list of n_j sites, where $y=x-\sum_{i=1}^{j-1} P_i n_i$ and k is the integer part of y/P_j+1 as

$$k = \left[\frac{y}{P_j} + 1 \right]. \quad (3)$$

After performing the process j on the site in the k th position in the list, the time is advanced by dt and the lists are updated. We simulate systems with sizes 50^2 and 100^2 , but in the following we show results obtained for the larger system with a size 100^2 , since the larger system has smaller fluctuation.

III. WITHOUT DIFFUSION

From our previous works on a homogeneous system [13,17] the nonlinear autocatalysis with a finite k_2 is found essential for the chiral symmetry breaking, whereas the linear autocatalysis k_1 is inefficient. Therefore, k_1 is set absent hereafter: $k_1=0$. In order to find out the effect of diffusion, we consider in this section the development of chirality in space without the material transport. The effect of diffusion is studied in the next section. Here, the order of chiral symmetry breaking is studied as a function of the strength of the nonlinear autocatalysis or of the concentration of active molecular species.

A. Chiral symmetry breaking as a function of nonlinear autocatalysis

First, we consider the k_2 dependence of the chiral symmetry breaking, when the whole lattice sites are occupied by chemically active species: $c=1$. When the nonlinear autocatalytic effect is strong enough such as $k_2=100k_0$ with $\lambda=k_0$, achiral reactants A quickly transform to chiral species R or S . Therefore, even by starting from an achiral initial configuration with only achiral reactants A , domains of R and S are formed in the early stage, as shown at a time $k_0 t=50$ in Fig. 2. Then, the domain competition sets in and those domains surrounded by another type shrink as shown in the middle column in Fig. 2. Eventually, competition ends up by the dominance of one enantiomeric type, S in the case shown in the right column of Fig. 2. In some cases the system decouples into two interpenetrating domains of R and S , both of which in effect extend to infinity due to the periodic boundary conditions in the x and y directions: Then, it takes

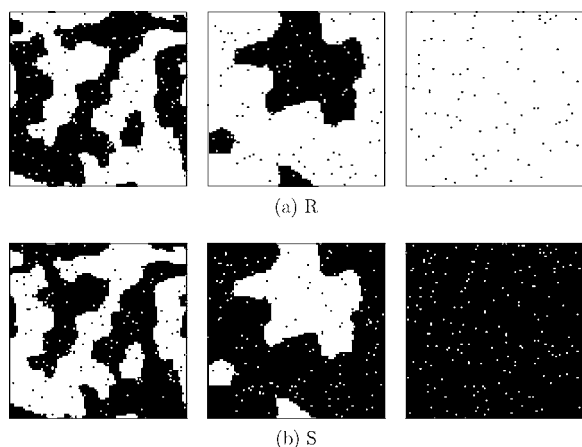


FIG. 2. Configuration evolution of (a) *R* and (b) *S* molecules in a diffusionless system. Times are $k_0t=50, 250, 1750$ from left to right. Parameters are $k_0=\lambda$, $k_1=0$, $k_2=100k_0$ with $c=1$, and the system size is 100^2 .

an enormous time until the minor domain extinguishes and the system accomplishes the final equilibrium state.

In order to obtain the equilibrium value of the order parameter ϕ in a reasonable simulation time, therefore, we start simulations from an initial configuration with a complete chiral order such that the whole lattice sites are occupied by *R* (or *S*) species. Equilibrium states are readily realized from this initial configuration, and the equilibrium value of the order parameter ϕ thus obtained is shown in Fig. 3 at various strengths of the nonlinear autocatalysis k_2/k_0 . Since the non-autocatalytic reaction k_0 drives the system to the racemic state, the value of the order parameter ϕ decreases as k_2 decreases and vanishes at a critical value of k_2/k_0 around 10: The system recovers the chiral symmetry, getting into the racemic state.

The qualitative features of domain competition shown in Fig. 2 and the emergence of symmetry breaking at large k_2 as shown in Fig. 3 suggest to us some resemblance with the phase transition in an Ising ferromagnet [19,20]. In fact, one may find some analogy of our reaction system to an Ising ferromagnet: In the latter, each lattice site is occupied by an Ising spin, which can be in one of the two states: up or down.

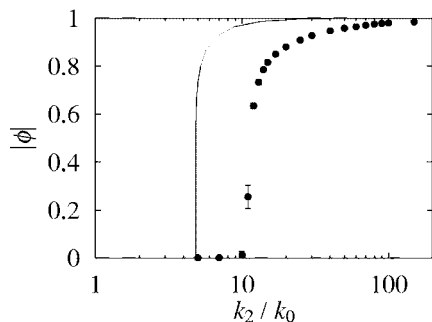


FIG. 3. Enantiomeric excess $|\phi|$ versus k_2/k_0 at the full occupation $c=1$ in a semilogarithmic plot. A curve represents the temperature dependence of the magnetization [21] of a square Ising model, where a temperature is related to the chemical reaction rates as $k_2/k_0=\exp(4J/k_B T)-1$.

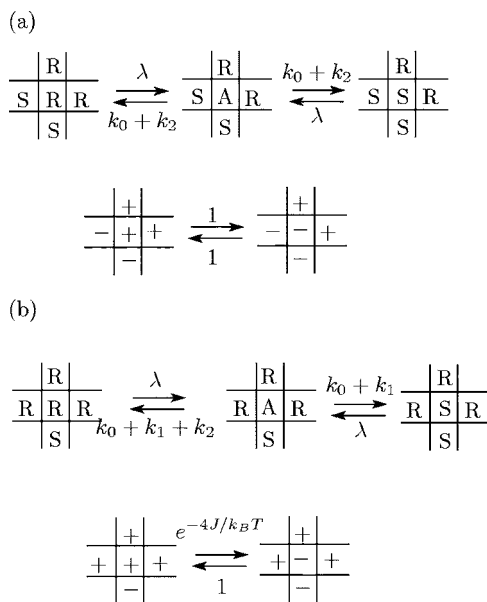


FIG. 4. Analogies of the state transition in the reaction model (above) and the Ising ferromagnet (below). (a) $n=2$ and (b) $n=3$.

When the members of a nearest-neighboring spin pair have the same orientation, the energy is low as given by $-J < 0$, whereas when the members of a pair are in opposite orientations, the energy is high as $J > 0$: The energy difference is set to be $2J > 0$. At a temperature T , a spin flips its orientation with a transition probability which depends on the associated energy change. Let the spin to flip have n nearest-neighboring spins with the same orientation. Then, it will have $4-n$ spins of the same orientation after the flip and we denote the transition probability as $W(n \rightarrow 4-n)$. In order to ensure thermal equilibrium asymptotically, it is known to be sufficient if the detailed balance condition between the transition probabilities of one process and its reverse

$$\frac{W(n \rightarrow 4-n)}{W(4-n \rightarrow n)} = \exp(-\Delta E/k_B T) \tag{4}$$

is satisfied, where $\Delta E=4(n-2)J$ represents an energy change. For example, when a site is surrounded by two up spins and two down spins, $n=2$ and the transition probability of an up spin to flip downward is equal to its reverse process, as shown in the lower row of Fig. 4(a). Then, in equilibrium the probability $P_+(2,2)$ of an up spin surrounded by two up spins and two down ones is equal to that of a down spin in the same environment $P_-(2,2)$: $P_+(2,2)=P_-(2,2)$. We associate, for instance, *R* and *S* molecules to the up and down Ising spins, respectively. Then, the transitions for $n=2$ in the Ising model correspond to transitions between an *R* and *S* molecule surrounded in the neighborhood by two *R*'s and two *S*'s [upper row of Fig. 4(a)]. Since the alternation of *R* and *S* is mediated by an achiral reactant *A*, the equilibrium probabilities of *R* and *S* in the configuration of Fig. 4(a) are related as $\lambda P_R(2,2)=(k_0+k_2)P_A(2,2)=\lambda P_S(2,2)$ and thus $P_R(2,2)=P_S(2,2)$, consistent with our assignment of *R* and *S* molecules to up and down spins. When a site is surrounded by three *R*'s and one *S* molecule as in the upper row of Fig.

4(b), the equilibrium probability that the site is occupied by an R molecule $P_R(3,1)$ is higher than the one by an S molecule $P_S(3,1)$. They are related as $\lambda P_R(3,1) = (k_0 + k_2)P_A(3,1)$ and $k_0 P_A(3,1) = \lambda P_S(3,1)$, and thus $P_R(3,1) = (1 + k_2/k_0)P_S(3,1)$: At a lattice site surrounded by three R 's and an S , the probability of finding an R molecule is higher than that of finding an S molecule by a factor $(1 + k_2/k_0)$. For the Ising system, the corresponding situation is the spin on the site surrounded by three up's and one down: $n=3$. The relation between probabilities that a site is occupied by an up spin and by a down is $e^{-4J/k_B T} P_+(3,1) = P_-(3,1)$ [see the lower row of Fig. 4(b)]. Thus, we may assume that the ratio $(1 + k_2/k_0)$ corresponds in the Ising model to the ratio of the transition probabilities $\exp(4J/k_B T)$. In other words, the nonlinear autocatalytic rate k_2 in our chiral model might correspond to the coupling constant of the two-dimensional Ising model as

$$k_2/k_0 = e^{4J/k_B T} - 1. \quad (5)$$

Since the numbers of R and S molecules correspond to those of up and down spins in the Ising ferromagnet, the chiral order parameter ϕ corresponds to the spontaneous magnetization M of the Ising model. The latter is exactly known to behave as [21] $M = [1 - \sinh(2J/k_B T)^{-4}]^{1/8}$. By using relation (5), the magnetization M is plotted in Fig. 3 by a solid curve.

The transition temperature T_c of the Ising model on the square lattice is exactly known to be at $k_B T_c / 2J = 1/\ln(1 + \sqrt{2}) \approx 1.135$ [20]. Thus in the present reaction model chiral symmetry breaking is expected to take place at $k_2 \geq k_{2c} = 2(\sqrt{2} + 1)k_0 \approx 4.83k_0$. However, the order parameter ϕ obtained by simulations decreases faster than the Ising magnetization as k_2 decreases: For the chiral symmetry breaking a larger value of the nonlinear autocatalysis $k_2 \approx 10k_0$ is required, as shown in Fig. 3. This is because of the approximate nature of the relation between the Ising coupling constant J and the nonlinear autocatalytic rate k_2 . The production rate in our model is independent of the number of neighboring R (S) species as far as it is more than 2, whereas transition rate to the up spin state in an Ising model increases as the neighboring number of up spins increases: This means that our coupling constant k_2 is effectively weaker than the Ising coupling parameter. Also the existence of an achiral species is not included in the Ising model. The decomposition process from a chiral species R or S back to an achiral reactant A induces fluctuation which breaks ordering, and a chirally ordered state in our reaction model is less stable than the ferromagnetic state in the Ising ferromagnet: The strong nonlinearity is necessary for the symmetry breaking. In fact, the critical value for the chiral symmetry breaking k_{2c} depends on the decomposition rate λ , though the k_2 versus J relation in Eq. (5) is independent of λ . From simulations with a large $\lambda = 10k_0$, the order is found to be easily broken at $k_{2c} \approx 23k_0$, whereas for small $\lambda = 0.1k_0$ the order holds until $k_{2c} \approx 9k_0$.

B. Dilution effect on chiral symmetry breaking

We now keep the nonlinear autocatalytic effect as strong as $k_2/k_0 = 100$ and consider the dilution effect ($c < 1$) on the

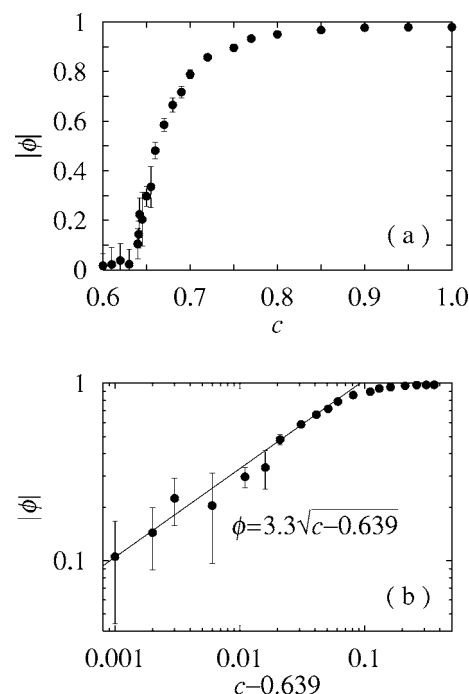


FIG. 5. Enantiomeric excess $|\phi|$ versus c in a diffusionless system with a strong nonlinear autocatalysis $k_2/k_0=100$.

chiral symmetry breaking. If there is no material transport, the behavior of the system depends strongly on the arrangement of vacant sites. Therefore, in order to obtain the order parameter ϕ we average nine samples at concentrations lower than $c=0.7$, whereas three samples are sufficient at higher concentrations with error bars less than a symbol size. As the system is diluted, the probability that active chemical species are contiguous to each other decreases. In the present reaction model, however, a reactant A should be surrounded by chiral products R or S to sustain the autocatalysis. Therefore, the chiral symmetry breaking is possible only at concentrations at least larger than the site percolation threshold of the square lattice $c_p=0.592746$ [22,23]. Below c_p , chemically active species can form only clusters of a finite size and the chiralities of these clusters are independent of each other. Therefore, the system cannot be in a single state. The order parameter ϕ actually decreases as the system is diluted, as shown in Fig. 5(a), and the system becomes racemic at concentrations lower than the critical value $c_c(D=0)$. By assuming a critical concentration at $c_c(D=0) \approx 0.639$, the order parameter ϕ shows a power-law dependence $\phi \propto \sqrt{c - c_c(D=0)}$, as shown in Fig. 5(b). The critical concentration $c_c(D=0)$ without diffusion is close to but larger than c_p .

A discrepancy between $c_c(D=0)$ and c_p might be understood by using the similarity of the present diluted reaction model to a site-diluted Ising ferromagnet, where lattice sites are diluted substitutionally by nonmagnetic impurities [24]. In a site-diluted Ising model, the transition temperature is known to decrease as the concentration of nonmagnetic impurity increases and the phase transition vanishes at the critical concentration close to the percolation threshold c_p [25]: The transition temperature is zero at the critical concentration. If relation (5) holds, however, our reaction model with

$k_2=100k_0$ corresponds to an Ising ferromagnet at a finite temperature $k_B T/2J=0.433$ or $T/T_c=0.38$. A thermal fluctuation favors the recovery of the symmetry even if a percolating cluster exists, and this may be the reason that the critical concentration $c_c(D=0)$ is larger than the percolation threshold c_p .

IV. DIFFUSION ENHANCEMENT OF THE CHIRALITY SELECTION

We now study the diffusion effect on the chirality selection in a diluted system. The transport of material in general increases the chance for an achiral reactant A to meet chiral products R and S in their lifetimes, and may enhance the autocatalytic effect. When the diffusion is extremely fast, the system becomes homogeneous: This case will be studied in the following subsection analytically. With a finite diffusion coefficient, numerical simulation is the only possible method to study and the results so obtained will be analyzed by an interpolation formula in the second subsection. Temporal evolution of the system is also influenced by the diffusion process, and the acceleration in the development of the chiral order is discussed in the last subsection.

A. Homogeneous case with $D=\infty$

When the diffusion is extremely fast, the system becomes homogeneous. Then, the simple mean-field approximation leads to the rate equations for the homogeneous concentrations:

$$\begin{aligned}\dot{r} &= k(r)a - \lambda r, \\ \dot{s} &= k(s)a - \lambda s,\end{aligned}\quad (6)$$

with the rate constant $k(r)=k_0+4k_1r+6k_2r^2$. Here in this subsection we restore the rate k_1 of the linear autocatalytic reaction, in order to be general. The factors $4r$ and $6r^2$ represent the probabilities that at least one or two of the four neighboring sites are occupied by R species, respectively, in the sense of the mean-field approximation. Since the system is assumed to be closed, the total concentration of chemically active species satisfies the conservation law $a+r+s=c=\text{const}$. Then, the total concentration of chiral products $u=r+s$ is shown to vary as

$$\dot{u} = [2k_0 + 4k_1u + 3k_2u^2(1 + \phi^2)](c - u) - \lambda u, \quad (7)$$

whereas the order parameter ϕ evolves as

$$\dot{\phi} = \frac{c-u}{u} \phi [-2k_0 + 3k_2u^2(1 - \phi^2)]. \quad (8)$$

Since $0 \leq u \leq c$, Eq. (8) is similar to the time-dependent Landau equation with nontrivial fixed points if $u^2 > 2k_0/(3k_2)$. The other point to remark is that Eq. (8) does not depend explicitly on the linear autocatalytic rate k_1 ; ϕ depends on k_1 only implicitly through u . Thus the linear autocatalysis alone cannot break the chiral symmetry in the present model.

The equilibrium values of u and ϕ are calculated from the algebraic equations given by $\dot{\phi}=\dot{u}=0$. The spontaneous chi-

ral symmetry breaking takes place at a critical concentration $c_c(D=\infty)$ when the diffusion is infinitely fast: The order parameter ϕ of a homogeneous system takes a finite value for $c_c(D=\infty) < c \leq 1$. For $k_1=0$ the order parameter ϕ is explicitly written as a function of the concentration c as

$$\phi^2 = 1 - \frac{6k_0k_2}{\lambda^2} \left(c - \sqrt{c^2 - \frac{2\lambda}{3k_2}} \right)^2 \quad (9)$$

and the critical concentration is calculated to be $c_c(D=\infty) = (4 + \lambda/k_0)/\sqrt{k_0/24k_2}$. It takes the value $c_c(D=\infty)=0.1020$ for the parameter values $k_1=0$, $k_2=100k_0$, and $\lambda=k_0$.

B. Finite diffusion constant

The emergence of chiral order at a finite vacancy diffusion is studied by the Monte Carlo simulation. It is found that the symmetry breaking takes place rather rapidly even if we start from a completely achiral initial configuration with all the chemically active molecules being achiral reactants A as $a=c$: The order parameter approaches quickly the asymptotic value, though which enantiomer dominates over the other is determined randomly in each simulation run. Therefore, in the following we initiated simulations from the complete achiral state with only A and V species.

The steady-state value of ee or $|\phi|$ at various values of diffusion coefficient D is shown as a function of the concentration of active species c by symbols in Fig. 6(a). A solid curve in the left extreme represents relation (9) for a homogeneous system with $D=\infty$. The most striking feature is that the ϕ - c relations at different D 's look similar but with shifts to the lower-concentration side as D increases. The D dependence of the shift might be considered in the following way. The chiral products R or S diffuse in an area of about D/λ sites during the lifetime $1/\lambda$. Therefore, in a system where diffusion is allowed the effective density of chiral catalysts is enhanced by a factor $1+AD/\lambda$ in comparison to the system without diffusion. A proportionality constant A will be determined later by fitting to the simulation results. With a very large diffusion D , however, there will be overlappings of various diffusion areas and the diffusive enhancement may saturate. Thus, even with an infinitely fast diffusion, a finite concentration of active species is necessary, as is given by Eq. (9).

The diffusive enhancement of the effective concentration means that in order to reach a fixed value of the order parameter ϕ , the required concentration of active species $c(\phi;D)$ for a system with a finite diffusion coefficient D can be less than $c(\phi;D=0)$ for a diffusionless system. Here we propose a simple formula for $c(\phi;D)$ interpolating between the diffusionless limit $c(\phi;D=0)$ and the homogeneous limit $c(\phi;D=\infty)$ as

$$c(\phi;D) = \frac{c(\phi;0) + c(\phi;\infty)(AD/\lambda)}{1 + (AD/\lambda)}, \quad (10)$$

where $c(\phi;0)$ is obtained by the simulation [Fig. 5(a)], whereas $c(\phi;\infty)$ is obtained by solving Eq. (9) as

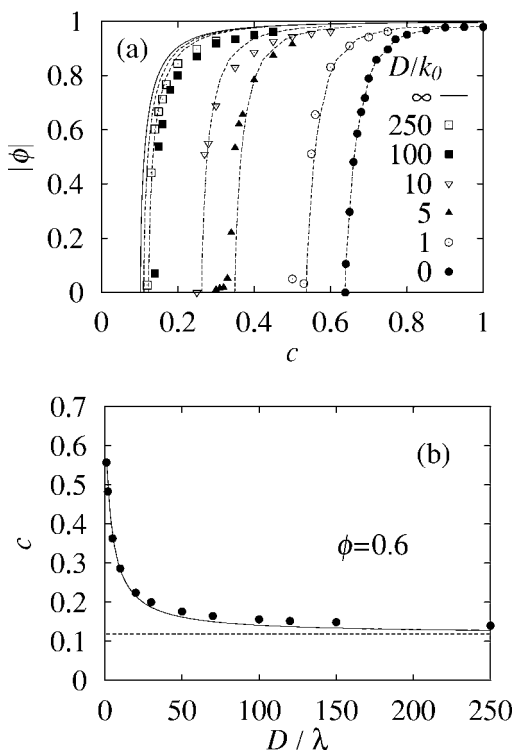


FIG. 6. (a) Enantiomeric excess $|\phi|$ versus c at various values of the diffusion coefficient D/k_0 . The reaction parameters are $k_2/k_0 = 100$, $k_1 = 0$, and $\lambda = k_0$. A solid curve represents relation (9) for a homogeneous system. Dashed curves represent interpolation (10) at various diffusion coefficients. (b) Diffusion coefficient dependence of the concentration c where the order parameter takes the value $\phi = 0.6$. A curve represents the interpolation (10) with a parameter $A = 0.235$. The dotted line represents the homogeneous case with $c(0.6; D = \infty) = 0.118$.

$$c(\phi; \infty) = \frac{1}{\sqrt{24k_0k_2}} \left(\lambda \sqrt{1 - \phi^2} + \frac{4k_0}{\sqrt{1 - \phi^2}} \right). \quad (11)$$

To determine the constant A , we fit formula (10) with simulation data at $\phi = 0.6$. The reason for the choice of a nonzero value of ϕ is that the value of $c(\phi; D)$ is expected to be more accurate away from the transition point, $\phi = 0$. The fit gives the value $A \approx 0.235$ and agrees well at small D but deviates systematically at large D , as shown in Fig. 6(b).

With this value of A , we interpolate the whole ϕ - c curve for arbitrary D by Eq. (10), as is drawn by dashed curves in Fig. 6(a). The trend of the down shifting in the concentration as the diffusion increases is well reproduced, even though the fitting is not perfect, especially at a large diffusion coefficient D . There, we have so far no plausible theory on the D dependence of $c(\phi; D)$.

C. Time development of chirality selection

So far we discussed on the diffusional amplification of saturation values of the order parameter ϕ , but the time dependence of $\phi(t)$ is also influenced by the diffusion process [18]. A few examples of the time evolution of ϕ are shown in Fig. 7(a) with various values of a diffusion constant D/k_0 .

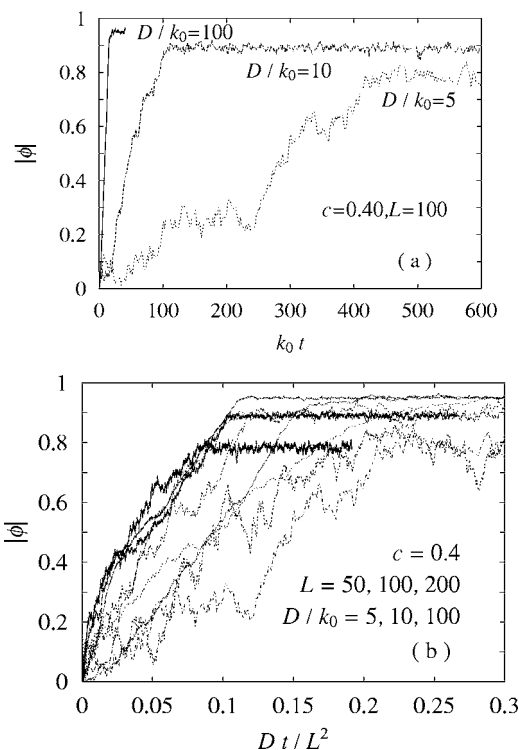


FIG. 7. Time evolution of the order parameter ϕ starting from an achiral initial condition with only A species with a concentration $c = 0.40$. (a) For a system with a size $L = 100$ but with different diffusion constant D and (b) for systems with different D 's and sizes L . The time is scaled as Dt/L^2 in (b).

The initial solution consists of only achiral reactant A with a concentration $c = 0.4$ in a system with a size $L^2 = 100^2$. The chiral order develops, but the speed as well as the saturation value depend on the diffusion coefficient D . In general, the order ϕ develops rapidly with a large D even though the evolution is stochastic with fluctuations. After a rapid and almost linear increase of ϕ , it saturates and fluctuates around the equilibrium value. Since the diffusive transport in a time t extends in a region of a radius \sqrt{Dt} [26], the establishment of the order within a system of a size L requires a time $t \sim L^2/D$. Therefore, in terms of the scaled and dimensionless time Dt/L^2 , the order parameter ϕ should behave similarly, irrespective of the diffusion constant D and the system size L . This scaling behavior is indeed observed as shown in Fig. 7(b) for $D/k_0 = 5, 10$, and 100 and $L = 50, 100$, and 200 . Nevertheless, the overlapping of ϕ in Fig. 7(b) is not perfect, because each time evolution is controlled by individual initial nucleation of the dominant chiral species. For example, for a system with a size 100^2 with a diffusion constant $D/k_0 = 5$, the duration of the initial nucleation stage is so long as shown in Fig. 7(a) that the front propagation by diffusion takes place quite late.

V. SUMMARY AND DISCUSSIONS

We study diffusion effect on the chirality selection during a chemical production of chiral molecules R or S from an achiral reactant A in a solution by means of a square lattice

model. In addition to the usual reactions of the production and the decomposition of chiral species, autocatalytic processes are incorporated such that an achiral reactant surrounded by many enantiomers of one type increases the turnover rate to that type. Specifically, the nonlinear autocatalysis which takes place when the reactant is surrounded by two or more enantiomers of one type is found to be essential in the chiral symmetry breaking.

When all the lattice sites are occupied by chemically active species A , R , or S , the spontaneous symmetry breaking has some similarity to the phase transition of an Ising ferromagnet. The strength of the nonlinear autocatalysis k_2 in our chemical model is approximately related to the ferromagnetic coupling constant. The chemical model at very large k_2 evolves through the domain competition, similar to the dynamics of the Ising model at low temperatures. As k_2 decreases, the chiral order extinguishes, but earlier than the expectation from the Ising model. The discrepancy may be due to the larger degrees of freedom: three in the chemical model whereas two in the Ising model.

Inclusion of vacancies or dilution suppresses the degree of the chiral symmetry breaking or the enantiomeric excess ϕ , and below the critical concentration of chemically active species, the system is in a racemic state with a chiral symmetry. In a diffusionless system ($D=0$) with a strong nonautocatalysis, the system is similar to the site-diluted Ising model, and the critical concentration is close to but larger than the percolation threshold c_p .

Diffusion enhances the chiral order ϕ , since the migration of chiral products enhances the chance of molecular collision and the autocatalytic process as well. In the limit of an infinitely fast diffusion ($D=\infty$), the system behaves as if it is

homogeneous and the rate equation in the mean-field approximation describes the chiral symmetry breaking: The steady-state solution is obtained analytically in this limit. At a finite diffusion coefficient D , the concentration dependence of ϕ is shifted from the diffusionless limit ($D=0$) to the homogeneous limit ($D=\infty$). The behavior is interpreted as the diffusive enhancement of concentrations of chiral species and is summarized in an interpolation formula of c dependence of ϕ or $c(\phi;D)$ between the two limits.

Diffusion accelerates the time development of the chirality selection as well. After the initial stage of nucleation of chiral clusters and a competition between them, a dominant cluster grows via the diffusion process. For a nonconserved order parameter, in general, the effect of diffusion extends in a region of a linear size \sqrt{Dt} in a time t , and thus the enantiomeric excess ϕ increases almost linearly proportional to t in two dimensions. In a finite system of a linear dimension L , ϕ saturates in a time of order L^2/D . In fact, in terms of a dimensionless time Dt/L^2 , the ee ϕ behaves similarly irrespective of the diffusion constant D and the system size L . This scaling behavior is already proposed and confirmed in the analysis of a slightly different model by means of partial differential equations [18], and our Monte Carlo simulation study is in accordance with it, except for the initial nucleation stage. If the material transport is mediated by hydrodynamic flow, the time evolution of the ee is expected to be much faster, as is confirmed numerically in Ref. [18]. Since the area of the Earth is large but nevertheless of a limited size, our analysis of the chiral order propagation in a system of a finite size may shed some illuminating light on the chirality selection of life on Earth.

-
- [1] W. A. Bonner, *Origins Life Evol. Biosphere* **21**, 407 (1992).
 [2] D. Kondepudi and I. Prigogine, *Modern Thermodynamics* (Wiley, Chichester, 1998).
 [3] D. K. Kondepudi and K. Asakura, *Acc. Chem. Res.* **34**, 946 (2001).
 [4] S. F. Mason and G. E. Tranter, *Proc. R. Soc. London, Ser. A* **397**, 45 (1985).
 [5] D. K. Kondepudi and G. W. Nelson, *Nature (London)* **314**, 438 (1985).
 [6] W. J. Meiring, *Nature (London)* **329**, 712 (1987).
 [7] F. C. Frank, *Biochim. Biophys. Acta* **11**, 459 (1953).
 [8] P. G. H. Sandars, *Origins Life Evol. Biosphere* **33**, 575 (2003).
 [9] A. Brandenburg, A. Andersen, M. Nilsson, and S. Höfner, *Origins Life Evol. Biosphere* **35**, 225 (2005).
 [10] K. Soai, T. Shibata, H. Morioka, and K. Choji, *Nature (London)* **378**, 767 (1995).
 [11] I. Sato, D. Omiya, K. Tsukiyama, Y. Ogi, and K. Soai, *Tetrahedron: Asymmetry* **12**, 1965 (2001).
 [12] I. Sato, D. Omiya, H. Igarashi, K. Kato, Y. Ogi, K. Tsukiyama, and K. Soai, *Tetrahedron: Asymmetry* **14**, 975 (2003).
 [13] Y. Saito and H. Hyuga, *J. Phys. Soc. Jpn.* **73**, 33 (2004).
 [14] Y. Saito and H. Hyuga, *J. Phys. Soc. Jpn.* **74**, 1629 (2005).
 [15] R. Plasson, H. Bersini, and A. Commeyras, *Proc. Natl. Acad. Sci. U.S.A.* **101**, 16733 (2004).
 [16] M. Le Bellac, F. Mortessagne, and G. G. Batrouni, *Equilibrium and Non-Equilibrium Statistical Thermodynamics* (Cambridge University Press, Cambridge, England, 2001).
 [17] Y. Saito and H. Hyuga, *J. Phys. Soc. Jpn.* **73**, 1685 (2004).
 [18] A. Brandenburg and T. Multamaki, *Int. J. Astrobiol.* **3**, 209 (2004).
 [19] E. Ising, *Z. Phys.* **31**, 253 (1925).
 [20] L. Onsager, *Phys. Rev.* **65**, 117 (1944).
 [21] C. N. Yang, *Phys. Rev.* **85**, 808 (1952).
 [22] D. Stauffer, *Introduction to Percolation Theory* (Taylor & Francis, London, 1985).
 [23] R. M. Ziff, *Phys. Rev. Lett.* **69**, 2670 (1992).
 [24] R. B. Stinchcombe, in *Phase Transition and Critical Phenomena*, edited by C. Domb and J. L. Lebowitz (Academic, New York, 1983), Vol. 7, p. 151.
 [25] Z. Néda, *J. Phys. I* **4**, 175 (1994).
 [26] S. Chandrasekhar, *Rev. Mod. Phys.* **15**, 1 (1943).